Lyapunov approach to synchronization of chaotic systems with vanishing nonlinear perturbations: From static to dynamic couplings

Paolo Arena, Arturo Buscarino, and Luigi Fortuna
DIEEI, University of Catania, Viale A. Doria 6, Catania 95125, Italy
and CNR-IASI, Istituto di Analisi del Sistemi e Informatica "A. Ruberti," 00185 Rome, Italy

Luca Patanè*
Dipartimento di Ingegneria Università degli Studi di Messina, Contrada di Dio, 98166 Messina, Italy

(Received 27 March 2020; revised 30 April 2020; accepted 26 June 2020; published 15 July 2020)

Synchronization of chaotic dynamics can be pursued by means of different coupling strategies. Definitely, master-slave coupling represents one of the most adopted solutions, even if it presents some limitations due to the coupling term's selection strategy. In this paper, we investigate the role of different structures of coupling terms on the synchronization properties of master-slave chaotic system configurations. Here, Lyapunov theory for linear systems with nonlinear vanishing perturbations is exploited. The obtained results allow to determine the capability of a static, dynamic, or mixed coupling connection in stabilizing the synchronization manifold, using linear techniques based on the root locus. This knowledge allows to design the coupling structure considering also the synchronization error transient features, which are, here, shown to improve in the presence of higher-order dynamic couplings. A number of cases of study, involving classical chaotic nonlinear systems, show the efficacy and simplicity of the application of the strategy proposed.

DOI: 10.1103/PhysRevE.102.012211

I. INTRODUCTION

Synchronization of chaotic systems is a deeply studied research topic, initially theoretically formalized and experimentally demonstrated using circuits implementation [1]. Nowadays, we can find applications of synchronization in several fields including biological phenomena [2], secure communications [3,4], and robotic system control [5,6].

The synchronization phenomenon, i.e., the coherent motion of two or more chaotic units starting from different initial conditions, can be formalized as complete, phase, or phase lag synchronization, antisynchronization, and many other weaker levels of synchronization [7–9]. Different methods and techniques are currently used for synchronization control, such as distributed adaptive control, intermittent control, impulsive control, and others [10–12].

In our paper, we will tackle the problem of complete synchronization of chaotic systems under master-slave coupling. This occurs when two identical systems are connected with a unidirectional coupling: One system (i.e., the master) drives the response of the other (i.e., the slave) [13,14]. Here, negative feedback is commonly adopted: A linear combination of the slave state variables is fed back generating an error signal with respect to the master dynamics, whose action induces synchronization in the slave system. The error signal can be directly inserted in the slave system as a driving signal or can be processed by a dynamic controller.

The problem of synchronization with dynamic linear feedback control has been already addressed in literature at the aim to overcome limitations in static schemes. Recently [15], a chaotic system was analyzed as a multimode linear system, and the root locus technique was applied to design the appropriate loop gain. Moreover, the use of a linear dynamic controller, designed solving a constrained nonlinear optimization problem for systems in Lur'e form, was discussed in Ref. [16]. In Ref. [17], Lyapunov stability theory and Gerschgorin's theorem were used to determine necessary conditions to get synchronization, verifying the accuracy by means of numerical simulations. Linear matrix inequalities were used to design an integral dynamic coupling in Ref. [18], whereas Refs. [19,20] focus on the application of Lyapunov theory for perturbed systems to analyze the synchronization of chaotic systems. More recently, in Ref. [21], the use of dynamic coupling was investigated in the synchronization of hyperchaotic systems.

The role of dynamic coupling assumes a further interesting perspective in connection to reservoir computing-based networks. In echo-state networks (ESNs) [22], standard sigmoidal functions without any time dependence were first adopted as activation functions of internal nodes. To include time features, leaky integrator neuron (LIN) models were considered. The LIN role resembles the effect of the dynamic coupling, here, proposed for a master-slave synchronization scheme. It was demonstrated that LINs improve the ESN performance both in recognizing strongly time-warped dynamical patterns and in learning relatively slow and noisy time series [23]. ESN stability can be computed using Lyapunov exponents [24] and Lyapunov

*Author to whom correspondence should be addressed: lpatane@unime.it

functions [25], strategies taken into consideration in the proposed
paper.

In this paper, following Refs. [19,21], we introduce a formal generalization of the master-slave configuration, considering either static or dynamic coupling and the combination of them. In particular, we determine a strategy to assess which master-slave configuration is able to guarantee and enhance complete synchronization on the basis of the specific chaotic dynamics. The strategy is based on the application of Lyapunov theory for systems with vanishing perturbations [26] employing the root locus to design the coupling configuration and the corresponding coupling gain. The proposed approach allows to obtain synchronization also in cases where the mere static coupling fails. A further interesting property, here, investigated is the effect of the selected coupling scheme on the reduction of the transient time needed to reach complete synchronization. In particular, the introduction of higher-order coupling systems can be envisaged if the synchronization performances in terms of convergence time need to be improved.

The paper is organized as follows: In Sec. II, the framework defining the generalized master-slave configuration with static and/or dynamic coupling is introduced, in Sec. III, the discussion of the coupling schemes in terms of control systems is outlined. Static and dynamic coupling are deeply investigated in Sec. IV, whereas the effectiveness of a mixed static-dynamic coupling is introduced in Sec. V. Finally, conclusions are drawn in Sec. VI.

II. MASTER-SLAVE SYSTEMS WITH STATIC AND DYNAMIC COUPLING: PRELIMIARIES

The general master-slave coupling scheme adopted for chaos synchronization is, here, reported. The dynamic evolution of the state variables of a master-slave system can be represented as

$$\begin{aligned} \dot{\mathbf{x}}_M &= \mathbf{F}(\mathbf{x}_M), \\ \mathbf{y}_M &= \mathbf{C}\mathbf{x}_M, \\ \dot{\mathbf{x}}_S &= \mathbf{F}(\mathbf{x}_S) + \mathbf{k}\mathbf{B}(\mathbf{y}_M - \mathbf{y}_S), \\ \mathbf{y}_S &= \mathbf{C}\mathbf{x}_S, \end{aligned} \tag{1}$$

where $\mathbf{x}_M$, $\mathbf{y}_M$, $\mathbf{x}_S$, and $\mathbf{y}_S$ are the state and output variables of the master and slave systems, respectively, $\mathbf{F}$ is generally a nonlinear function representing the dynamics of each system, $\mathbf{B} \in \mathbb{R}^{nx1}$ and $\mathbf{C} \in \mathbb{R}^{1xn}$ are the input and output vectors, respectively (n is the order of each system), and $\mathbf{k} \in \mathbb{R}$ is the strength of the unidirectional coupling.

We have complete synchronization between master and slave when the state error dynamics tends to zero,

$$\lim_{t\to\infty} e_{M-S}(t) = \lim_{t\to\infty} [\mathbf{x}_M(t) - \mathbf{x}_S(t)] = 0. \tag{2}$$

When the coupling is performed only between the ith component of the master state vector and the jth component of the slave one, the coupling term can be rewritten as

$$\mathbf{k}\mathbf{B}(\mathbf{y}_M - \mathbf{y}_S) = \mathbf{k}\mathbf{B}\mathbf{C}e_{M-S}, \tag{3}$$

where the matrix $\mathbf{BC} \in \mathbb{R}^{nxn}$ is a zeros matrix with a single element equal to one.

For chaotic systems, this coupling mechanism was successfully adopted in literature, and the suitable values of k, able to guarantee synchronization, can be found using the master stability function (MSF) which provides necessary conditions from the calculation of the largest Lyapunov exponent transverse to the synchronization manifold [27]. Since the MSF depends only on the single system dynamics and on the coupling scheme, general considerations can be gained for given chaotic systems coupled through specific variables. In literature, three possible behaviors of the MSF have been characterized with respect to the coupling strength [28]. In type I MSF, synchronization cannot be reached for any value of the coupling strength, in type II MSF, a minimum coupling strength among which synchronization is achievable, can be found, whereas in type III MSF, the coupling strength must fall in a given range. Under this perspective, the search for strategies able to allow for synchronization in cases, such as type I MSF, are worth being investigated. An interesting case is represented by the Rössler oscillator where a synchronized dynamics can be found, for a specific interval of the coupling gain (i.e., type III MSF), when $\mathbf{B} = [1\ 0\ 0]^T$ and $\mathbf{C} = [1\ 0\ 0]$, whereas, when $\mathbf{B} = [1\ 0\ 0]^T$ and $\mathbf{C} = [0\ 1\ 0]$, that corresponds to a configuration where the error between the master and the slave second state variables is fed into the first equation of the slave system, it is not possible to find a synchronized regime, acting on the coupling gain (i.e., type I MSF) [29].

Recently, to overcome this limit, a linear dynamic coupling was proposed and applied to synchronize harmonic oscillators, chaotic, and hyperchaotic systems [1,19,21]. The dynamic controller acts as a filtering system that mediates the error between master and slave. When a first order dynamical system is adopted for the coupling, Eq. (1) can be generalized as

$$\begin{aligned} \dot{\mathbf{x}}_M &= \mathbf{F}(\mathbf{x}_M), \\ \dot{\mathbf{x}}_S &= \mathbf{F}(\mathbf{x}_S) - \mathbf{B}\mathbf{x}_C, \\ \dot{\mathbf{x}}_C &= -\alpha\mathbf{x}_C - \mathbf{k}\mathbf{C}(\mathbf{x}_M - \mathbf{x}_S), \end{aligned} \tag{4}$$

here, $\mathbf{x}_C$ is the state variable of the linear dynamic coupling and $\alpha \in \mathbb{R}_+$ is a parameter accounting for the dynamics of the coupling system. The coupling system can be further extended including higher-order dynamics, for instance, considering a second order mass-spring-damper-like system. Therefore, the formulation of Eq. (4) can be generalized defining a state matrix for the coupling dynamics $\mathbf{H} \in \mathbb{R}^{mxm}$ where m is the order of the coupling system. In this case, the dimensions of matrices $\mathbf{B} \in \mathbb{R}^{nxm}$ and $\mathbf{C} \in \mathbb{R}^{mxn}$ will change accordingly.

Stability analysis

The stability of the synchronization manifold can be analyzed using different approaches among which the master stability function [29] and the Lyapunov theory for perturbed systems [26].

The Lyapunov approach guarantees sufficient conditions for the stability of the synchronization error dynamics and allows to analyze the problem considering a restriction of the system dynamics to the linear part, handling the remaining nonlinear dynamics as a vanishing perturbation.

Under these assumptions, we can reformulate the synchronization error dynamics as follows:

$$\dot{\mathbf{e}}_{M-S} = (\mathbf{A} - \mathbf{kBC})\mathbf{e}_{M-S} + \mathbf{g}(t, \mathbf{e}_{M-S}), \tag{5}$$

where $\mathbf{A}$ is the state matrix associated with the linear components of the error dynamics and $\mathbf{g}(t, \mathbf{e}_{M-S})$ contains all the nonlinearities present in the error system. Therefore, we can define the state matrix of the error dynamics, restricted to the linear part, when a static coupling is applied to the master-slave configuration as follows:

$$\tilde{\mathbf{A}} = \mathbf{A} - \mathbf{kBC}. \tag{6}$$

Equation (5) can be extended in the presence of a dynamic coupling considering a generalized error vector $\tilde{\mathbf{e}} = [\mathbf{e}\,\mathbf{x}_C]^T$, a perturbation $\tilde{\mathbf{g}}(t, \tilde{\mathbf{e}}) = [\mathbf{g}(t, \mathbf{e})\,\mathbf{O}_{1m}]^T$, and the state matrix in Eq. (6) can be extended considering a block matrix,

$$\tilde{\mathbf{A}} = \begin{bmatrix} \mathbf{A} & \mathbf{B} \\ -\mathbf{kC} & \mathbf{H} \end{bmatrix}. \tag{7}$$

The stability of the extended error system needs to be imposed to synchronize master and slave. Following the theory of stability for perturbed systems [26], we can consider the linear dynamics as associated with the nominal system, whereas the nonlinear parts are treated as a vanishing perturbation. Under these assumptions, a sufficient condition to guarantee a stable synchronization manifold is derived imposing the stability of the linear system, i.e., matrix $\tilde{\mathbf{A}}$ is Hurwitz and verifying that the perturbation is vanishing $\tilde{\mathbf{g}}(t, \mathbf{O}_{1(n+m)}) = \mathbf{O}_{1(n+m)}$. Finally, considering $\tilde{\mathbf{g}}(t, \tilde{\mathbf{e}})$ as a continuous nonlinear function, we need to impose a linear growth bound satisfying the following Lipschitz condition: $\|\tilde{\mathbf{g}}(t, \tilde{\mathbf{e}})\|_2 \leqslant \gamma \|\tilde{\mathbf{e}}\|_2$, $\forall t \geqslant 0$, $\forall \tilde{\mathbf{e}} \in D \subset \mathbb{R}^{n+m}$. The parameter γ needs to verify the following inequality $\gamma < 1/[2\lambda_{\max}(\mathbf{P})]$, where $\mathbf{P}$ is the symmetric positive definite matrix that satisfies the Lyapunov equation $\mathbf{P}\tilde{\mathbf{A}} + \tilde{\mathbf{A}}^T\mathbf{P} = -\mathbf{I}$ as commented in Ref. [26]. If these properties are verified, the origin is a stable equilibrium point for the error system, guaranteeing a complete synchronization between master and slave.

III. EFFECTS OF THE COUPLING SYSTEMS

The principles of master-slave synchronization, discussed in Sec. II, can be applied to generic nonlinear dynamical systems, in particular, to chaotic ones. This system category is characterized by an extreme sensitivity to initial conditions, and the synchronization property is a key aspect in several applications [4,5]. For the sake of simplicity, here, we will take into consideration autonomous chaotic dynamical systems with a single output variable that corresponds to one of the state variables and the control action will be applied only on a single equation of the slave system, therefore, matrices $\mathbf{B}$ and $\mathbf{C}$ will contain zeros with the exception of a single element equal to one, whose position identifies the configuration of the master-slave coupling. However, the following analysis can be extended also in the presence of generic input and output matrices.

We will start analyzing the effect of static and dynamic couplings in terms of asymptotic stability of the linear system defined by state matrix $\tilde{\mathbf{A}}$. We can perform this analysis with different methods, a possible strategy consists in applying the Routh-Hurwitz criterion to the characteristic polynomial associated with the state matrix as depicted in Ref. [19]. In our paper, we followed another route that allows to formalize the problem from a different perspective, thus, helping understand the role of the dynamical coupling.

A. Static coupling

The characteristic polynomial of matrix $\tilde{\mathbf{A}}$ when a static coupling is applied is, here, reported

$$p_{\tilde{\mathbf{A}}}(\lambda) = |(\mathbf{A} - \lambda\mathbf{I}) - k\mathbf{BC}|, \tag{8}$$

where $|\cdot|$ indicates the determinant operator. Applying the matrix determinant lemma, we can rewrite Eq. (8),

$$p_{\tilde{\mathbf{A}}}(\lambda) = |(\mathbf{A} - \lambda\mathbf{I})| - k\mathbf{C}[\mathbf{A} - \lambda\mathbf{I}]_{\text{adj}}\mathbf{B}, \tag{9}$$

where $[\cdot]_{\text{adj}}$ represents the adjugate matrix operator. With the assumptions, previously introduced, on the type of the input and output matrices, we can reformulate Eq. (9),

$$p_{\tilde{\mathbf{A}}}(\lambda) = p_{\mathbf{A}}(\lambda) - k\bar{p}^A_{i,j}(\lambda), \tag{10}$$

where $\bar{p}^A_{i,j}(\lambda)$ is the term with position (i, j) in matrix $[\mathbf{A} - \lambda\mathbf{I}]_{\text{adj}}$ with i and j corresponding to the position of the nonzero element in the output and input matrices, respectively. In the following, we use the notation $i \to j$ to identify the coupling connection where the error between master and slave ith state variables is used as input for the jth equation of the slave system.

From Eq. (10), it is evident that the effect of the static coupling consists in an additive term to the characteristic polynomial of the noncontrolled error system. The term $\bar{p}^A_{i,j}(\lambda)$ could be either a constant or a polynomial, modulated by the gain k, depending on the selected coupling variables.

B. Dynamic coupling

In the presence of a dynamic coupling, the previous analysis can be applied as long as a further step is initially performed. In fact, for a generic block matrix $\mathbf{M}$, the determinant can be calculated using the property of the Schur complement [30],

$$\mathbf{M} = \begin{bmatrix} M_1 & M_2 \\ M_3 & M_4 \end{bmatrix} \quad |\mathbf{M}| = |M_4|\left|M_1 - M_2M_4^{-1}M_3\right|, \tag{11}$$

with $\mathbf{M}_4$ nonsingular.

Applying this property, starting from the block matrix in Eq. (7), we can evaluate the characteristic polynomial of the controlled error system in the presence of a linear dynamic coupling as

$$p_{\tilde{\mathbf{A}}}(\lambda) = |\mathbf{H} - \lambda\mathbf{I}||(\mathbf{A} - \lambda\mathbf{I}) + k\mathbf{B}(\mathbf{H} - \lambda\mathbf{I})^{-1}\mathbf{C}|. \tag{12}$$

In this case, we have the product of two determinants: The former depends on the linear coupling system that we need to choose stable to guarantee the stability of the error system, therefore, we can concentrate on the the latter term that we want to express in the form reported in Eq. (8). If we suppose a first order dynamic coupling, the term $(\mathbf{H} - \lambda\mathbf{I})^{-1}$ is a scalar value, and we can move it outwards in the gain position. When a higher-order coupling system is considered, we can assume that only the equation associated with the last

state variable of the dynamical coupling system will receive the error information to control the slave system [19]. Under this assumption, the input matrix $\mathbf{B} \in \mathbb{R}^{n\times m}$ will be a zero matrix with a single element equal to one in position (j, m) and, similarly, the output matrix $\mathbf{C} \in \mathbb{R}^{m\times n}$ will contain a one in position (m, i), where m is the order of the coupling system.

Applying these constraints, it is simple to verify that the term we are interested in, for the matrix $(\mathbf{H} - \lambda\mathbf{I})^{-1}$, is that one in position (m, m). Therefore, Eq. (12) becomes

$$p_{\tilde{\mathbf{A}}}(\lambda) = p_{\mathbf{H}}(\lambda)\left[p_{\mathbf{A}}(\lambda) - k\bar{p}^{A}_{i,j}(\lambda)\frac{-\bar{p}^{H}_{m,m}(\lambda)}{p_{\mathbf{H}}(\lambda)}\right]. \tag{13}$$

As already underlined for the static coupling, also in the presence of a dynamic coupling, the characteristic polynomial of the controlled error system contains an additive term that, in general, is a ratio of polynomial functions. When the coupling system is characterized by a simple first order linear dynamics $\mathbf{H} = [-\alpha] \in \mathbb{R}$ and $-\bar{p}^{H}_{m,m}(\lambda)/p_{\mathbf{H}}(\lambda) = \frac{1}{\lambda+\alpha}$.

A careful analysis of Eqs. (10) and (13) for the static and dynamic couplings, respectively, leads to formulate the problem in terms of a feedback control scheme where the gain k is in both cases a parameter that influences the closed loop pole positions on the complex plane. These need to lie within the real negative half complex plane to satisfy the Lyapunov stability theory for perturbed systems applied to the master-slave synchronization problem. The stability of the error dynamics can be, therefore, studied using the well known root locus, thus, simplifying the overall procedure as illustrated in the following sections. For the sake of clarity and for consistency with the control theory standard notation, we will use the s variable instead of λ in the following analyses.

IV. STATIC AND DYNAMIC COUPLING IN CHAOTIC SYSTEM SYNCHRONIZATION

The master-slave synchronization scheme is, here, applied to the Rössler oscillator to underline strengths and weaknesses of the static coupling mechanism and the possible solutions introduced with the dynamic coupling.

A. Static coupling

An interesting case of study for the application of the proposed method is represented by the Rössler oscillator [31] characterized by the following dynamical equations:

$$\begin{aligned}\dot{x} &= -y - z,\\ \dot{y} &= -x + ay,\\ \dot{z} &= -cz + xz + b,\end{aligned} \tag{14}$$

where a, b, and c are positive parameters, fixed for the following simulations to $a = 0.2$, $b = 0.2$, and $c = 5.7$.

Formulating the problem of a master-slave synchronization of two identical Rössler chaotic systems, we can define state matrix $\mathbf{A}$ of the error system and the nonlinear perturbation term,

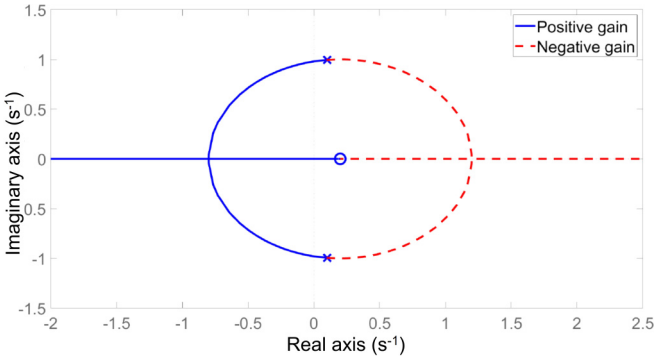

FIG. 1. Root locus associated with Rössler systems with a static coupling and configuration $1 \rightarrow 1$.

$$\mathbf{A} = \begin{bmatrix}0 & -1 & -1\\ 1 & a & 0\\ 0 & 0 & -c\end{bmatrix} \quad \mathbf{g}(t, \mathbf{e}_{M-S}) = \begin{bmatrix}0\\ 0\\ x_M z_M - x_S z_S\end{bmatrix}. \tag{15}$$

As previously illustrated in Ref. [20], to demonstrate that the nonlinear components act as a vanishing perturbation, we can rewrite $\mathbf{g}(t, \mathbf{e}_{M-S})$ through the components of the error vector $\mathbf{e}_{M-S} = [e_1\ e_2\ e_3]^T$,

$$\mathbf{g}(t, \mathbf{e}_{M-S}) = [0 \quad 0 \quad x_M e_3 + z_M e_1 - e_1 e_3]^T, \tag{16}$$

where it is easy to verify the vanishing condition $\mathbf{g}(t, \mathbf{O}_{1\times 3}) = \mathbf{O}_{1\times 3}$.

The characteristic polynomial of matrix $\mathbf{A}$ can be easily evaluated

$$p_A(s) = -(s + c)(s^2 - as + 1). \tag{17}$$

We can now evaluate the adjugate matrix of $\mathbf{A} - s\mathbf{I}$,

$$[\mathbf{A} - \mathbf{sI}]_{\text{adj}} = \begin{bmatrix}(s-a)(s+c) & -(s+c) & -(s-a)\\ s+c & s(s+c) & -1\\ 0 & 0 & s^2 - as + 1\end{bmatrix}. \tag{18}$$

Let us consider a static coupling with a connection configured as $1 \rightarrow 1$: The error between master and slave on the first state variables is used as input for the first equation of the slave system. On the basis of the considerations reported in Sec. III, we can analyze the root locus of the following system:

$$\begin{aligned}S^{1\rightarrow 1}_{\text{Static}}(s) &= -\frac{\bar{p}^{A}_{1,1}(s)}{p_A(s)}\\ &= \frac{-(s-a)(s+c)}{-(s+c)(s^2 - as + 1)}\\ &= \frac{(s-a)}{(s^2 - as + 1)}.\end{aligned} \tag{19}$$

We can now verify the effect of the control gain in terms of stability evaluating the root locus for the system $S^{1\rightarrow 1}_{\text{Static}}(s)$ as shown in Fig. 1. There is a range for the coupling gain $0.2 < k < 5$ where the system is stable.

The last condition to be verified is related to the linear growth bound for the perturbation. To evaluate the parameter γ, we need to solve the Lyapunov equation $\mathbf{P}\tilde{\mathbf{A}} + \tilde{\mathbf{A}}^T\mathbf{P} =$

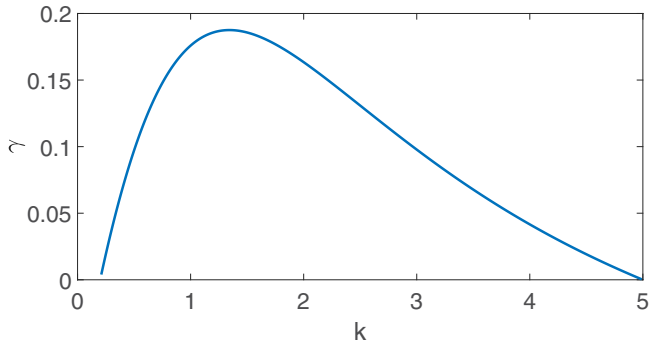

FIG. 2. Relation between the parameter γ related to the linear growth bound for the perturbation and the coupling gain k in the Rössler systems with static coupling and configuration $1 \rightarrow 1$.

$-\mathbf{I}$. Matrix $\tilde{\mathbf{A}}$ can be calculated as in Eq. (6) considering that a static coupling with a connection of the type $1 \rightarrow 1$ corresponds to an input matrix $\mathbf{B} = [1\ 0\ 0]^T$ and an output matrix $\mathbf{C} = [1\ 0\ 0]$. The relation between the parameter γ and the coupling gain k is shown in Fig. 2.

We can select the coupling gain in correspondence to the maximum of the curve: $k \simeq 1.34$ and $\gamma \simeq 0.1875$. Therefore, to verify the linear growth bound, we need to satisfy the following equation:

$$|x_M e_3 + z_M e_1 - e_1 e_3| - 0.1875\|e_{M-S}\|_2 < 0. \tag{20}$$

The analytical verification of this condition $\forall\, t \geqslant 0$ and $\forall\, e_{M-S} \in D \subset \mathbb{R}^3$ is beyond the aims of this paper. For the Rössler system, we performed a numerical analysis, identifying if this inequality is verified in regions surrounding a series of points on the trajectory followed by the master system as illustrated in Fig. 3. Here, the domains for the state variables of the slave system, that verify inequality in Eq. (20), is reported. The visual representation of the domains is restricted to a cube with side dimensions equal to 2, centered on selected points of the master trajectory. It has to be noted that the domains reported in Fig. 3 are not always dense, therefore, during the system dynamic evolution, the condition could be locally violated.

A typical outcome of the static coupling scheme with the selected gain is reported in Fig. 4 where the time evolution

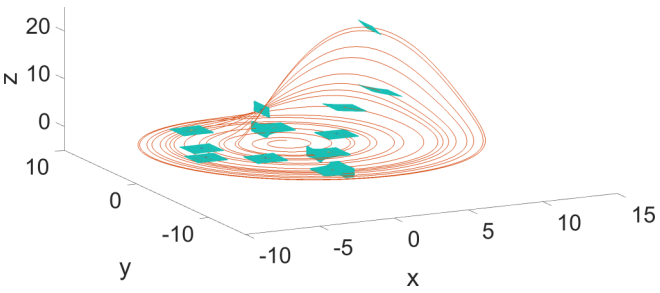

FIG. 3. For each selected point of the master trajectory, the domain for the slave system where Eq. (20) is verified is depicted. To facilitate visualization, the analysis was restricted to a cube with sides equal to 2 and centered in the chosen point for the master.

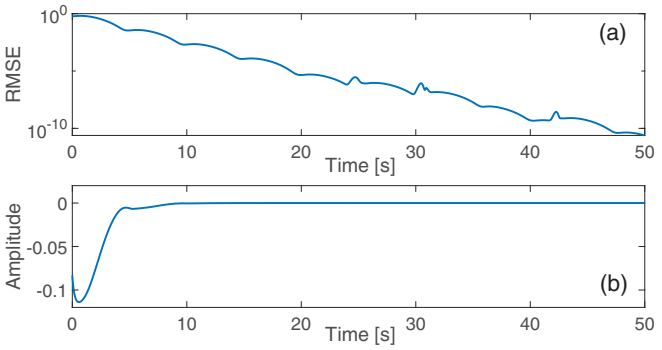

FIG. 4. Typical dynamics obtained in a master-slave synchronization scheme for two identical Rössler systems with static coupling and configuration $1 \rightarrow 1$: (a) root mean square error (RMSE) between the master and the slave state variables; (b) first term of Inequality (20).

of the synchronization error and the linear growth bound condition for the perturbation are shown.

The concurrent verification of the three conditions introduced in Sec. II A guarantees a sufficient condition for the master-slave synchronization. In particular, that one imposing the linear growth bound for the perturbation has been evaluated in the worst case [26] and, even if it could not be verified somewhere on the phase plane, however, the synchronization manifold can still be contractive. Interesting results are reported in Ref. [32] where a comparison between the proposed approach and the master stability function applied to Chua's circuit is provided.

B. Dynamic coupling

The dynamic coupling can be applied either to synchronize systems when the static coupling is not able to solve the problem or to improve the synchronization properties of the systems.

Referring to the Rössler oscillator, let us consider a case different from that one treated in Sec. IV A where the first state variable is no longer available and we need to apply the coupling configuration $2 \rightarrow 1$. As discussed in Ref. [29] and further investigated in Ref. [19], this configuration does not guarantee a stable synchronization manifold independently on the selected coupling gain k.

This appears evident if we evaluate the equivalent of Eq. (19). In this case,

$$\begin{aligned} S^{2\rightarrow 1}_{\text{Static}}(s) &= -\frac{\tilde{p}^A_{2,1}(s)}{p_A(s)} \\ &= \frac{-(s+c)}{-(s+c)(s^2 - as + 1)} \\ &= \frac{1}{(s^2 - as + 1)}. \end{aligned} \tag{21}$$

The root locus obtained for this system, reported in Fig. 5(a), shows that all the poles never belong contemporarily to the stable region. Here, we demonstrate that the inclusion of a dynamic coupling can modify this portrait. A simple first

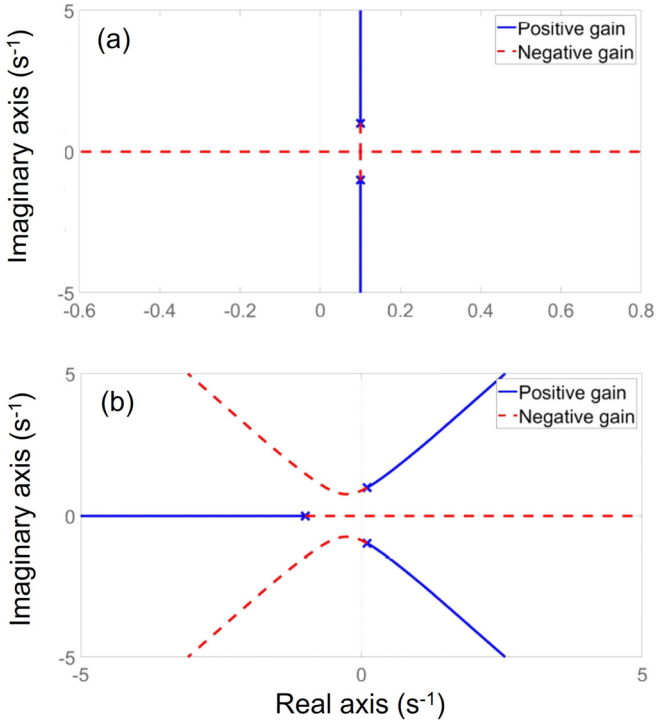

FIG. 5. Master-slave Rössler systems with configuration $2 \rightarrow 1$: Root locus associated with a static coupling in (a) and first order dynamic coupling with $\alpha = 1$ in (b).

order dynamic coupling ($\mathbf{H} = [-\alpha]$) leads to

$$S_{\mathrm{DynI}}^{2\rightarrow 1}(s) = \frac{-\bar{p}_{2,1}^{A}(s)}{p_A(s)} \frac{-\bar{p}_{1,1}^{H}(s)}{p_H(s)} = \frac{-(s+c)}{-(s+\alpha)(s+c)(s^2-as+1)} = \frac{1}{(s+\alpha)(s^2-as+1)}. \tag{22}$$

The corresponding root locus, obtained for this configuration [Fig. 5(b)], clearly demonstrates the possibility to stabilize the system in a specific range of the coupling gain. Assigning, for instance, the parameter $\alpha = 1$, we can evaluate that, for $-1 < k < -0.36$, the system is stable.

Deepening the role of the dynamic coupling, we can analyze the stability in terms of the parameters α and k in closed form, applying some properties of the root locus. To evaluate the value of k for which the real pole of the system passes from the negative to the positive real part, we can impose that the origin belongs to the negative locus,

$$k = -\left.\frac{D(s)}{N(s)}\right|_{s=0} = -(s+\alpha)(s^2-0.2s+1)|_{s=0} = -\alpha, \tag{23}$$

where $D(s)$ and $N(s)$ are the denominator and numerator of the $S_{\mathrm{DynI}}^{2\rightarrow 1}(s)$ transfer function. To evaluate the other boundary, we need to verify when the other two complex poles enter on the left semiplane. When the order of the denominator (m_D) and the order of the numerator (m_N) verify the condition m_D-$m_N \geqslant 2$ the barycenter of the locus is independent from k, therefore, the sum of the real parts of the closed loop poles is

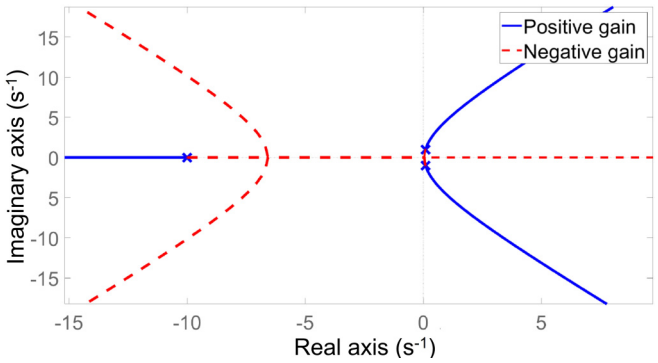

FIG. 6. Master-slave Rössler systems with configuration $2 \rightarrow 1$: Root locus associated with a first order dynamic coupling with $\alpha = 10$, and the system is always unstable independent from the coupling gain.

constant. In our case, we have three poles and no zeros, and the real parts of open loop poles are $[-\alpha,\ 0.1,\ 0.1]$. Imposing that two poles are crossing the imaginary axis, the position of the third one will be equal to the sum of the three in the open loop (i.e., $s = 0.2 - \alpha$). We can now apply the locus gain condition to this third pole,

$$\begin{aligned} k &= -\left.\frac{D(s)}{N(s)}\right|_{s=0.2-\alpha} \\ &= -(s+\alpha)(s^2-0.2s+1)|_{s=0.2-\alpha} \\ &= -0.2(\alpha^2-0.2\alpha+1). \end{aligned} \tag{24}$$

To define the range of the stabilizing gain as a function of α,

$$-\alpha < k < -0.2(\alpha^2-0.2\alpha+1). \tag{25}$$

To guarantee a feasible range for k, the left term and the right one of Inequality (25) need to be as follows:

$$\begin{aligned} -\alpha &< -0.2(\alpha^2-0.2\alpha+1) \\ 0.2\alpha^2 - 1.04\alpha + 0.2 &< 0. \end{aligned} \tag{26}$$

The solution of Inequality (26) guarantees a stability region in the range of $0.2 < \alpha < 5$. Beyond these limits, the root locus changes, some branching points occur, and stability cannot be obtained. For instance, if $\alpha = 10$, independent of k, there is always, at least, one unstable pole (Fig. 6).

This closed-form solution, for the evaluation of the range of admissible parameters, permits to improve the analysis performed in Ref. [19] where the Routh-Hurwitz criteria is applied, in fact, we are now able to better understand which is the effect of the dynamic coupling and its limits.

We can also evaluate the role of parameters α and k in connection with parameter γ. Matrix $\tilde{\mathbf{A}}$, needed to solve the Lyapunov equation, can be calculated from Eq. (7) considering a dynamic coupling with a connection type $2 \rightarrow 1$ that corresponds to an input matrix $\mathbf{B} = [1\ 0\ 0\ 0]^T$ and an output matrix $\mathbf{C} = [0\ 1\ 0\ 0]$. The values assumed by parameter γ as a function of the coupling gains k and α are reported in Fig. 7.

The stability region assumes a shape that is limited by the conditions in Inequality (25) and, in this case, there is a maximum of $\gamma = 0.0308$ where $\alpha \simeq 0.9$ and $k \simeq -0.62$.

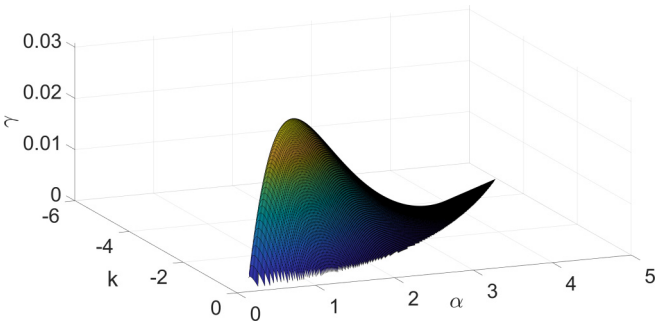

FIG. 7. Relation between the parameter γ related to the linear growth bound for the perturbation and the coupling parameters k and α in the Rössler systems with a first order linear dynamical coupling and configuration $2 \rightarrow 1$.

In Fig. 8, the evolution of the master and slave state variables together with the dynamical coupling variable are depicted, assuming, for the system parameters, the previous selected values. The considerations about the linear growth bound for the perturbation are similar to the previous case, and the time evolution of this condition is also reported in Fig. 8, last panel. It has to be noted that the state variable of the dynamical coupling system will contribute to the evaluation of $\|\tilde{\mathbf{e}}\|_2$. Simulations highlight some limited time windows, that correspond to a peak of the z variable where the condition on the linear growth bound for the perturbation is not verified. In fact, for a short time, a slight increment of the synchronization error occurs, but it is suddenly annihilated after a transient.

In addition, looking to the adjugate matrix in Eq. (18), it is easy to verify that, choosing as coupling configuration $1 \rightarrow 2$, we will have only a change in the sign with respect to the configuration $2 \rightarrow 1$. Following our analysis, we can conclude that, also in this case, the static coupling will not guarantee synchronization whereas a dynamical coupling will, just changing the sign of the coupling gain k with respect to the previous case.

Moreover, if we take into consideration the configurations $3 \rightarrow 1$ and $3 \rightarrow 2$, the presence of a zero element in the

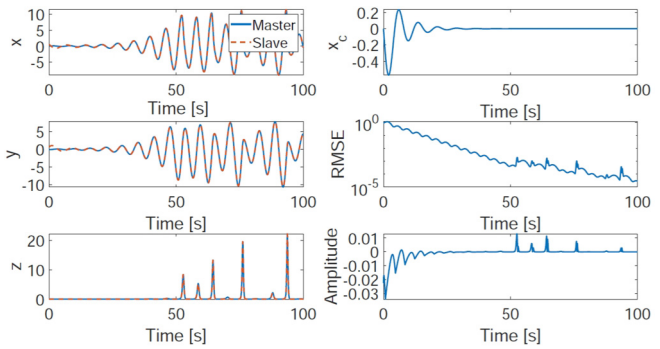

FIG. 8. Rössler systems with a first order linear dynamical coupling, (configuration $2 \rightarrow 1$, $\alpha = 0.9$, and $k = -0.62$): time evolution of the master and slave state variables (left panels) and dynamic coupling variable (top right panel); RMSE between the master and slave state variables and the condition in Eq. (20) with $\gamma = 0.0308$ are reported in the middle and bottom right panels, respectively.

adjugate matrix prevent to obtain, using the proposed approach, a stable synchronization manifold independent of the coupling system.

All these considerations provide useful indications to better understand the inherent complexity of the master-slave synchronization of chaotic systems. However, there are cases where, even if the proposed method is not able to find solutions, a stable synchronization manifold can occur as for the Rössler systems with configuration $3 \rightarrow 1$ as illustrated in Ref. [29] applying the master stability function. In this case, even if the dynamics of the linear part of the synchronization error is not stable, the nonlinear components, considered in our analysis as a perturbation on a stable dynamics, are, indeed, fundamental to stabilize the synchronization, pushing the evolution of the slave state variables in the direction that minimizes the error with the master.

C. Higher-order dynamic coupling

The introduction of a first order linear dynamical coupling system can guarantee a synchronization manifold where the static coupling fails. Here, we want to inspect whether the introduction of a higher-order coupling system could be useful. In Refs. [19,21], the possibility to augment the admissible range for the coupling gain, eliminating the upper bound was introduced, considering a second order dynamical system.

Moreover, the introduction of a higher-order dynamical coupling system can reduce the transient time of the synchronization regime by moving the position of the closed loop poles in the root locus, improving the performance of the synchronization scheme.

Considering the previous case of two Rössler systems with coupling configuration $2 \rightarrow 1$, we need, at least, a first order dynamical coupling (i.e., one pole) to guarantee a stable synchronization manifold, but, as demonstrated in Eqs. (25) and (26), there are strict limits on the parameters, and we are not able to freely move the dominant poles of the error system to speed up the error dynamics.

When a second order linear coupling system is considered, we introduce one zero and two poles that can help in stabilizing the error system. In fact, we can choose the following input, output, and state matrices for the coupling system:

$$\mathbf{H} = \begin{bmatrix} -\alpha & 1 \\ -\beta_1 & -\beta_2 \end{bmatrix} \quad \mathbf{B} = \begin{bmatrix} 0 & 1 \\ 0 & 0 \\ 0 & 0 \end{bmatrix} \quad \mathbf{C} = \begin{bmatrix} 0 & 0 & 0 \\ 0 & 1 & 0 \end{bmatrix}, \tag{27}$$

where α, β_1, and β_2 are control parameters. We fix one of the elements of matrix $\mathbf{H}$ to one because we do not need other parameters to arbitrarily place the zero and poles introduced by the linear dynamical coupling.

Applying this coupling system, we can rewrite Eq. (13),

$$p_{\tilde{\mathbf{A}}}(s) = p_{\mathbf{A}}(s) - k\, \bar{p}^{A}_{2,1}(s)\, \frac{s+\alpha}{s^2 + (\alpha+\beta_2)s + \beta_1 + \alpha\beta_2}. \tag{28}$$

With this second order coupling, we can move the dominant poles speeding up the error dynamics as reported in Fig. 9 where the root locus is reported adopting the following set of parameters for the matrix $\mathbf{H}$: $\alpha = 10$, $\beta_1 = 1600$, $\beta_2 = 90$. For this system configuration, if we consider a high coupling

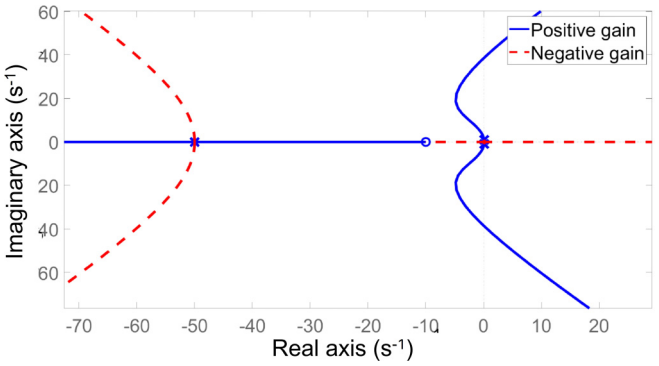

FIG. 9. Root locus associated with a second order dynamic coupling in a pair of Rössler systems with configuration $2 \rightarrow 1$ and parameters $\alpha = 10$, $\beta_1 = 1600$, $\beta_2 = 90$.

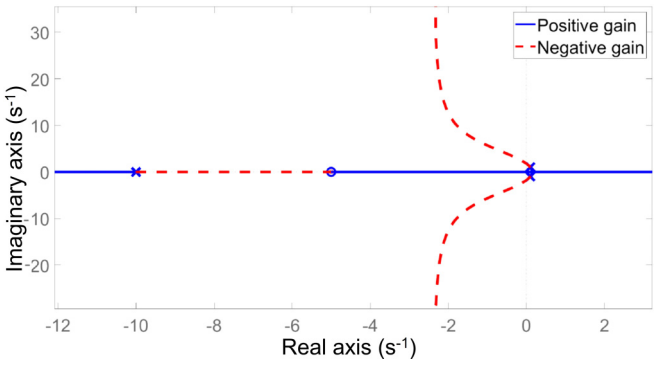

FIG. 10. Master-slave Rössler systems with configuration $2 \rightarrow 1$: root locus associated with a mixed static and dynamic coupling with $\alpha = 10$ and $k_S = -0.2$.

gain $k = 45 \times 10^3$, we can heavily reduce the transient time. A simulation campaign changing the initial conditions over 100 trials was carried out comparing the synchronization time in a pair of Rössler systems with first (parameters: $\alpha = 0.9$ and $k = -0.62$) and second order linear dynamical couplings as previously presented. Synchronization is reached when the RMSE between state variables is below a given threshold $E_{\text{Th}} = 0.001$. The obtained mean and standard deviation of the synchronization time for the two cases are as follows: $T_{\text{DynI}} = 78 \pm 17$ s and $T_{\text{DynII}} = 2 \pm 0.2$ s.

The possibility to reduce the transient time is an interesting property, and its relation with the selected coupling system is a relevant issue and will be deeply investigated in the future applications of the proposed methodology to better quantify the cost in terms of complexity and energy needed (e.g., increase in the coupling gain k) and the role of the nonlinear perturbation in providing limits to the transient time reduction.

V. MIXING STATIC AND DYNAMIC COUPLINGS

Following the previous analyses, we can investigate the effect of the combination of the static and dynamic couplings. In particular, as already demonstrated in Eqs. (22) and (28), a first order dynamical coupling system corresponds to the introduction of a single pole, whereas, a second order coupling is characterized by a system with one zero and two poles. Similarly, higher-order coupling schemes increase the number of poles and zeros. Trying to maintain the coupling system as simple as possible, another configuration that can be considered, consists of mixing static and first order dynamic couplings. This control solution produces an overall effect that corresponds to the following dynamical coupling:

$$H_{SD}(s) = k_S + \frac{1}{s+\alpha} = k_S \frac{s+z}{s+\alpha}, \tag{29}$$

where k_S is the additional gain we need to associate with the static coupling and can be chosen on the basis of the pole and zero positions. Therefore, we can impose $k_S = 1/(z-\alpha)$.

The effect of mixing static and dynamic couplings corresponds to introduce a zero-pole network that can be applied to move the center of the asymptotes in the root locus to improve the synchronization performances. This new coupling scheme is evaluated in the previously introduced Rössler oscillator and in the Hindmarsh-Rose (HR) neuron model.

A. Rössler oscillator

An interesting case of application of the proposed static and dynamic mixed strategy is related to the Rössler systems with coupling configuration $2 \rightarrow 1$. As previously demonstrated, we are able to produce a master-slave synchronization for a suitable range of the coupling gain when a dynamical coupling is considered. Herewith we want to demonstrate that, if we apply, at the same time, both a static and a dynamic coupling, we can obtain synchronization in an open region of the coupling parameter k. This possibility was previously investigated in Refs. [19,21] where, to solve this problem, a second order dynamical coupling was considered imposing parameters β_1 and β_2 as functions of the coupling gain k. The approach we are proposing simplifies the problem and provides a synthesis method through the study of the root locus. Figure 5(a) clearly shows that the static coupling is not able to stabilize the error system; we need to move the vertical asymptote to the left half-plane, and this can be performed introducing a zero-pole control network. Selecting the parameters $\alpha = 10$ and $k_S = -0.2$, we can impose a pole in -10 and a zero in -5; the effect of this coupling system is shown in Fig. 10. Analyzing the root locus, we can guarantee the stability of the linear error system, imposing only a lower bound limit to the coupling gain. The threshold value can be evaluated finding the intersection between the root locus and the imaginary axis,

$$k = -\left.\frac{D(s)}{N(s)}\right|_{s=-9.8} = -\left.\frac{(s+10)(s^2-0.2s+1)}{-0.2(s+5)}\right|_{s=-9.8} = -20.625. \tag{30}$$

Therefore, imposing a coupling gain $k < -20.625$ corresponds to an asymptotically stable error system. However, the proximity of the roots to the imaginary axis could be a problem in terms of convergence time, and due to the presence of the nonlinear perturbation a complete synchronization between master and slave cannot be guaranteed. Therefore, both acting on the coupling gain k and on the parameters α and k_S, we can move the closed loop position of the dominant poles towards more negative values that permit to reduce

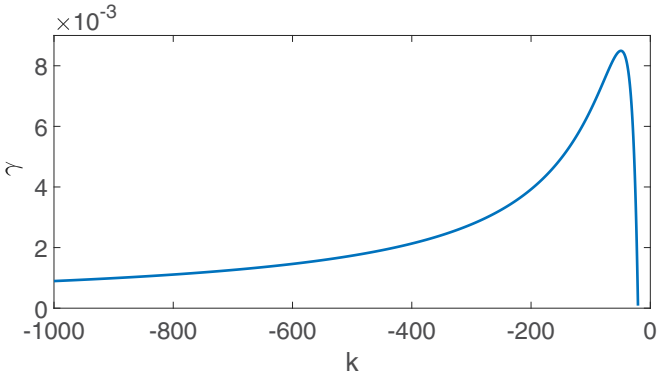

FIG. 11. Relation between parameter γ related to the linear growth bound for the perturbation and the coupling gain k in the Rössler systems with static coupling and configuration $2 \to 1$ when both static and first order dynamic couplings are applied.

the synchronization transient time creating a dynamics more robust to perturbations.

Analyzing the trend of parameter γ related to the linear growth bound for the perturbation as shown in Fig. 11, we can identify a peak for $k \simeq -49$ and an unlimited range of negative gain even if with a slightly stronger condition for the nonlinear component.

$$[\mathbf{A} - \mathbf{sI}]_{\text{adj}} = \begin{bmatrix} s^2 + \frac{503}{500}s + \frac{3}{500} & s + \frac{3}{500} & -s - 1 \\ 0 & s^2 + \frac{3}{500}s + \frac{3}{125} & 0 \\ \frac{3}{125}s + \frac{3}{125} & \frac{3}{125} & s^2 + s \end{bmatrix}. \tag{34}$$

We can verify the effect of the static coupling using the root locus as shown in Fig. 12. It can be noted that there are some configurations (i.e., $2 \to 1$ and $2 \to 3$) that due to the presence of a zero element in the adjugate matrix cannot be treated using the proposed approach. For the other configurations, we can distinguish a safe open region for the coupling gain (i.e., in the case of $2 \to 2$ where the increase in k will further stabilize the error system) and other cases

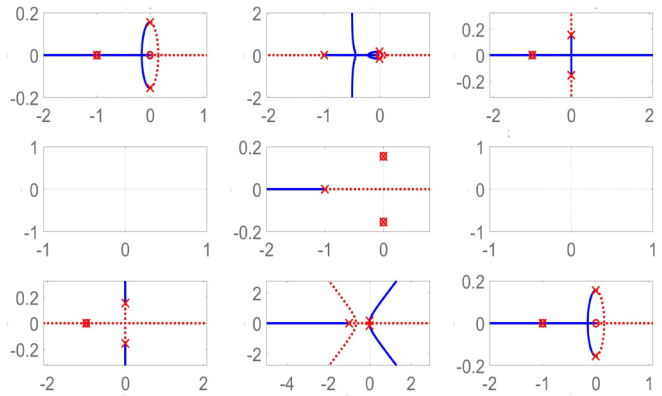

FIG. 12. Root locus associated with a static coupling in a master-slave HR neuron with all the possible configurations $i \to j$; the negative gain locus is reported using dashed lines.

B. HR neuron

The HR neuron is characterized by the following dynamical equations:

$$\begin{aligned} \dot{x} &= y - z - x^3 + 3x^2 + I \\ \dot{y} &= -y - 5x^2 + 1 \\ \dot{z} &= rsx - rz + 1.6rs \end{aligned} \tag{31}$$

where $I = 3.2$, $r = 0.06$, and $s = 4$. Also, in this case, it can be easily verified that the nonlinear part of the error system can be treated as a vanishing perturbation, therefore, we can analyze state matrix $\mathbf{A}$ of the linear part of the error system,

$$\mathbf{A} = \begin{bmatrix} 0 & 1 & -1 \\ 0 & -1 & 0 \\ rs & 0 & -r \end{bmatrix}. \tag{32}$$

The characteristic polynomial of matrix $\mathbf{A}$ can be easily evaluated

$$p_A(s) = -(s+1)(s^2 + 0.06s + 0.24). \tag{33}$$

For the HR neuron, the linear error system is already stable ($s_1 \simeq -1$, $s_{2,3} \simeq -0.03 \pm 0.49j$), but the poles are practically on the imaginary axis, and this condition is strengthened by the presence of the nonlinear perturbation.

We can now evaluate the adjugate matrix of $\mathbf{A} - s\mathbf{I}$,

where the proximity of the locus to the imaginary axis does not allow to identify a sharp behavior. In particular, if we consider the configuration $3 \to 1$ (and similarly $1 \to 3$), we identify a locus with a vertical asymptote, a case encountered also for the Rössler system with configuration $2 \to 1$. In this case, we move the position of the vertical asymptote towards the left semiplane, applying together the static and dynamic couplings. In fact, if we apply a first order dynamical coupling with $\alpha = 10$ and a static coupling with $k_S = -\frac{1}{5}$, we are introducing a zero-pole compensation network that modifies the root locus as shown in Fig. 13(a). The parameters selected for the coupling guarantee a shift of the dominant poles of the error system towards the stable region. When the coupling gain is not large enough ($k = -650$), synchronization does not occur, at least, in the selected time window ($t = 500$ s) as shown in Fig. 13(b). To guarantee a fast convergence, we can impose a higher negative gain as shown in Fig. 13(c) where the results obtained imposing $k = -3 \times 10^4$ are depicted.

By changing the value of the coupling gain and, consequently, the position of the closed loop poles in the root locus, it is possible to reduce the transient time as shown in Fig. 14. The presence of dominant poles with large negative real parts guarantees better performance whereas, moving towards the imaginary axis, enlarges the needed time window and reduces the basins of attraction due to the constraint on the nonlinear perturbation.

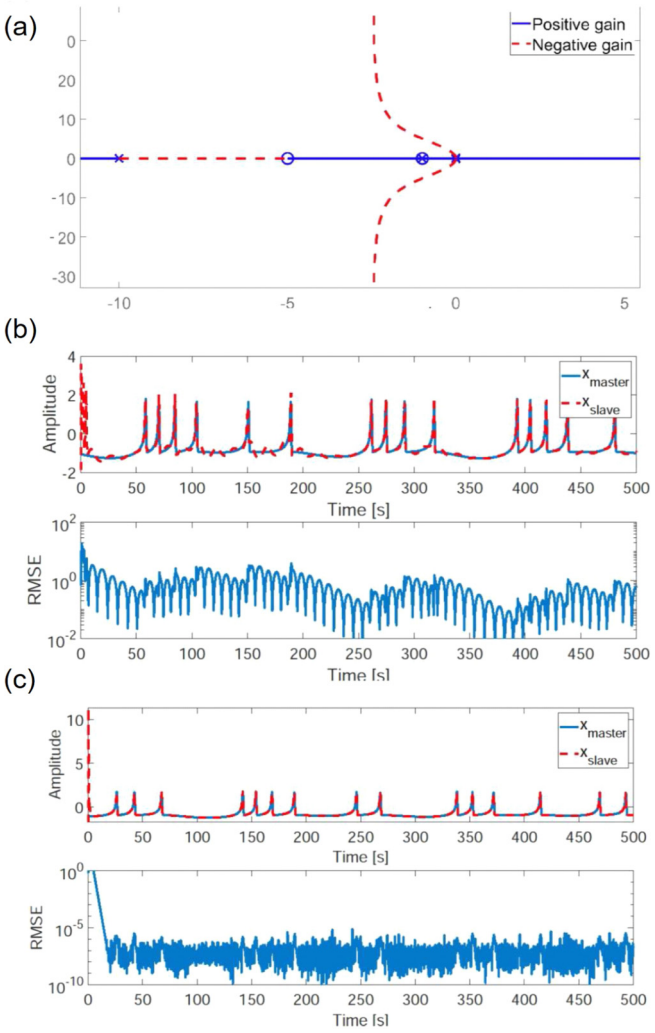

FIG. 13. Root locus associated with a mixed static and dynamic coupling in a master-slave HR neuron with configuration $3 \rightarrow 1$: (a) root locus with parameters $\alpha = 10$ and $k_S = -1/5$ and comparison between the x-state variables for the master and slave system together with the trend of the root mean square error for all state variables when (b) $k = -650$ and (c) $k = -3 \times 10^4$.

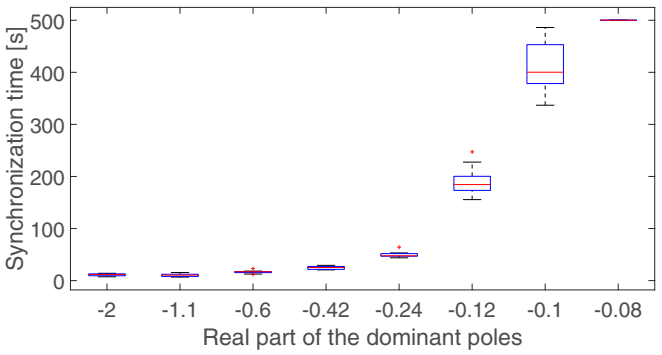

FIG. 14. Trend of the synchronization time considering a pair of HR neurons with configuration $3 \rightarrow 1$ changing the position of the dominant poles varying the coupling gain. The statistics is performed over 100 trials, for each case, changing the initial condition of the slave that spreads within a cube with side dimensions 2, centered on the master initial condition. The simulation time was fixed at 500 s. Simulations considering the most right and left cases are reported in Figs. 13(b) and 13(c), respectively.

VI. CONCLUSIONS

In this paper, a general framework for the design of master-slave coupling of nonlinear systems has been presented. The proposed approach relies on exploiting the Lyapunov theory for perturbed systems to determine the conditions under which a master-slave coupling either static and/or dynamic can lead to chaotic synchronization. This innovative approach represents a useful tool in the design of master-slave coupling, allowing to discriminate when, for a given chaotic dynamics, synchronization can be obtained on the basis of the available input and output signals. The outlined strategy provides guidelines to the analysis and synthesis of suitable coupling schemes. The application of the Lyapunov theory for perturbed systems allowed to consider the coupling as a linear system whose root locus for either positive or negative gains can be used to determine the coupling parameters, thus, generalizing the concept of feedback synchronization in chaotic systems.

Moreover, the relation between the adopted coupling system and the transient time needed to reach complete synchronization has been discussed underlying the possibility to use higher-order dynamical coupling systems to improve synchronization performances, even if an additional cost in terms of increase in the coupling gain is requested. This may represent a fundamental insight since, usually, the synchronization time is considered as a measure of the stability of the synchronous state [33]. Here, we provide a clear relationship between the coupling design and the time needed to reach the synchronous state, thus, allowing the synchronization time to be considered as a design specification. Nontrivial results on the adoption of static, dynamic, or combined static/dynamic coupling allowed to assess the validity of the approach and the suitability of the design guidelines in enhancing chaos synchronization in master-slave coupling.

[1] L. M. Pecora and T. L. Carroll, Synchronization in Chaotic Systems, Phys. Rev. Lett. **64**, 821 (1990).

[2] D. Sato, L.-H. Xie, A. A. Sovari, D. X. Tran, N. Morita, F. Xie, H. Karagueuzian, A. Garfinkel, J. N. Weiss, and Z. Qu, Synchronization of chaotic early afterdepolarizations in the genesis of cardiac arrhythmias, Proc. Natl. Acad. Sci. USA **106**, 2983 (2009).

[3] P. Arena, A. Buscarino, L. Fortuna, and M. Frasca, Separation and synchronization of piecewise linear chaotic systems, Phys. Rev. E **74**, 026212 (2006).

[4] K. Murali, Haiyang Yu, V. Varadan, and H. Leung, Secure communication using a chaos based signal encryption scheme, IEEE Trans. Consum. Electron. **47**, 709 (2001).

[5] G. Ren, W. Chen, S. Dasgupta, C. Kolodziejski, F. Wörgötter, and P. Manoonpong, Multiple chaotic central pattern generators with learning for legged locomotion and malfunction compensation, Inf. Sci. **294**, 666 (2015).

[6] X. Zang, S. Iqbal, Y. Zhu, X. Liu, and J. Zhao, Applications of chaotic dynamics in robotics, Int. J. Adv. Rob. Syst. **13**, 60 (2016).

[7] S. Boccaletti, J. Kurths, G. Osipov, D. Valladares, and C. Zhou, The synchronization of chaotic systems, Phys. Rep. **366**, 1 (2002).

[8] A. Pikovsky, M. Rosenblum, and J. Kurths, Phase synchronization in regular and chaotic systems, Int. J. Bifurcation Chaos **10**, 2291 (2000).

[9] C.-M. Kim, S. Rim, W.-H. Kye, J.-W. Ryu, and Y.-J. Park, Anti-synchronization of chaotic oscillators, Phys. Lett. A **320**, 39 (2003).

[10] W. Yu, P. DeLellis, G. Chen, M. di Bernardo, and J. Kurths, Distributed adaptive control of synchronization in complex networks, IEEE Trans. Autom. Control **57**, 2153 (2012).

[11] A. Bagheri and S. Ozgoli, Exponentially impulsive projective and lag synchronization between uncertain complex networks, Nonlinear Dyn. **84**, 2043 (2016).

[12] T. Huang, C. Li, W. Yu, and G. Chen, Synchronization of delayed chaotic systems with parameter mismatches by using intermittent linear state feedback, Nonlinearity **22**, 569 (2009).

[13] J. M. Cruz, M. Rivera, and P. Parmananda, Chaotic synchronization under unidirectional coupling: Numerics and experiments, J. Phys. Chem. A **113**, 9051 (2009).

[14] G.-P. Jiang and W. K. S. Tang, A global synchronization criterion for coupled chaotic systems via unidirectional linear error feedback approach, Int. J. Bifurcation Chaos **12**, 2239 (2002).

[15] K. Mistry, S. Dash, and S. Tallur, Synchronization of chaotic oscillators with partial linear feedback control, arXiv:1901.07770.

[16] J. A. K. Suykens, P. F. Curran, and L. O. Chua, Master-slave synchronization using dynamic output feedback, Int. J. Bifurcation Chaos **07**, 671 (1997).

[17] G.-P. Jiang, W. K.-S. Tang, and G. Chen, A simple global synchronization criterion for coupled chaotic systems, Chaos, Solitons Fractals **15**, 925 (2003).

[18] G.-P. Jiang, W. X. Zheng, W. K.-S. Tang, and G. Chen, Integral-observer-based chaos synchronization, IEEE Trans. Circuits Syst. II Express Briefs **53**, 110 (2006).

[19] J. Pena Ramirez, A. Arellano-Delgado, and H. Nijmeijer, Enhancing master-slave synchronization: The effect of using a dynamic coupling, Phys. Rev. E **98**, 012208 (2018).

[20] J. P. Ramirez, E. Garcia, and J. Alvarez, Master-slave synchronization via dynamic control, Commun. Nonlinear Sci. Numer. Simul. **80**, 104977 (2020).

[21] A. Buscarino, L. Fortuna, and L. Patanè, Master-slave synchronization of hyperchaotic systems through a linear dynamic coupling, Phys. Rev. E **100**, 032215 (2019).

[22] H. Jaeger and H. Haas, Harnessing nonlinearity: Predicting chaotic systems and saving energy in wireless communication, Science **304**, 78 (2004).

[23] H. Jaeger, M. Lukoševičius, D. Popovici, and U. Siewert, Optimization and applications of echo state networks with leaky-integrator neurons, Neural Networks **20**, 335 (2007).

[24] D. Verstraeten, B. Schrauwen, M. D'Haene, and D. Stroobandt, An experimental unification of reservoir computing methods, Neural Networks **20**, 391 (2007).

[25] A. Shirin, I. S. Klickstein, and F. Sorrentino, Stability analysis of reservoir computers dynamics via lyapunov functions, Chaos **29**, 103147 (2019).

[26] L. Khalil, *Nonlinear Systems* (Prentice-Hall, Upper Saddle River, NJ, 2002).

[27] L. M. Pecora and T. L. Carroll, Master stability functions for synchronized coupled systems, Int. J. Bifurcation Chaos **09**, 2315 (1999).

[28] S. Boccaletti, V. Latora, Y. Moreno, M. Chavez, and D. Hwang, Complex networks: Structure and dynamics, Phys. Rep. **424**, 175 (2006).

[29] L. Huang, Q. Chen, Y.-C. Lai, and L. M. Pecora, Generic behavior of master-stability functions in coupled nonlinear dynamical systems, Phys. Rev. E **80**, 036204 (2009).

[30] F. Zhang, *The Schur Complement and Its Applications* (Springer, Berlin, 2005).

[31] O. Rössler, An equation for continuous chaos, Phys. Lett. A **57**, 397 (1976).

[32] See Supplemental Material at http://link.aps.org/supplemental/10.1103/PhysRevE.102.012211 for a comparison between the proposed analysis based on the Lyapunov approach and the master stability function applied to Chua's circuit.

[33] P. J. Menck, J. Heitzig, N. Marwan, and J. Kurths, How basin stability complements the linear-stability paradigm, Nat. Phys. **9**, 89 (2013).